

Electromagnetic modelling of dielectric and metallic photonic crystals

D. Maystre, G. Tayeb, P. Vincent, S. Enoch, G. Guida

Institut Fresnel, Faculté des Sciences et Techniques de St Jérôme, case 262. Avenue Escadrille Normandie-Niemen. 13397 Marseille Cedex 20, France

1. INTRODUCTION

Photonic crystals have been the subject of considerable interest in the last decade. Many potential applications in technological areas such as the development of efficient semiconductor light emitters, filters, substrates for antennas in microwaves, lossless mirrors, have generated an intensive research in both experimental and theoretical domains. The properties of these structures depend strongly on the materials used. Dielectric crystals in general present transmission gaps limited to an octave or less while metallic crystals have a gap extending from a null frequency to a cut-off value. Metallic crystals are intended to be used in the microwaves region (antennas substrates for instance) whereas dielectric crystals are mainly devoted to the visible and infrared regions. Concerning the theoretical modelling of these structures, efficient techniques are now available in the one and two-dimensional cases. But the three-dimensional case leads to huge numerical problems, and it is not possible at the present time to deal with finite size structures sufficiently large to be realistic. This is the reason why it seems necessary to get a better knowledge of the intrinsic properties of these 3D structures. Homogenization techniques should be quite helpful, since they are able to replace a complex 3D photonic crystal by a homogeneous effective medium, which is much simpler to handle [1-4].

This paper presents two recent results obtained in our Laboratory using the electromagnetic theory [5-7]. The first one concerns metallic crystals. In the 2D case, we show that homogenization theory can predict with good accuracy the plasmon frequency of the crystal. Moreover, we compare the behaviors of 3D and 2D crystals, and we point out some similarities and some differences in their properties. The second part is related to the ultrarefractive property of 2D dielectric crystals [8]. This property appears at the edges of the gaps, and is closely related to the fact that near the gap the crystal simulates an effective medium with optical index close to zero. This phenomenon appears when the complex transmission of the crystal presents

rapid phase variations, and can give rise to surprising effects as anomalous translation shift or splitting of a limited beam.

2. METALLIC CRYSTALS

2.1 Modelling tools

In this section, we study metallic crystals made of very thin infinitely conducting wires lying in vacuum. Note that the infinitely conducting assumption is not so restrictive in the microwaves frequencies. The radius of the wires is r , and they are arranged periodically with a period d . Three different structures are studied, and we will call them 2D, 3D, and 3D-periodic crystals (fig. 1).

The 2D crystals are studied with the help of rigorous electromagnetic theories. In the case where the 2D crystal is periodic along x , we use a grating code based on an integral theory [5]. When the crystal is composed of a finite set of wires, we use a modal method based on scattering matrices, the fields being expressed as Fourier Bessel series [6].

The theory we use for the study of the 3D crystal [7] is based on the Electric Field Integral Equation (EFIE) proposed by Harrington for wire antennas [9]. Since the radius of the wires is assumed to be small compared to the wavelength, the unknown reduces to the intensity flowing in each wire. In the original work of Harrington, it is assumed that the intensity vanishes at a free extremity of a wire. We have shown that this assumption is not valid in the case of our study [7]. Consequently, our theory does not use this hypothesis. In the same way, we do not assume that Kirchhoff's law is satisfied at a junction between wires. Numerous checks have been performed in order to validate this approximate theory: energy balance and reciprocity, comparison with rigorous methods in the bidimensional case, and with another approximate method in the 3D case [10]. We found that the theory is quite reliable provided that r is less than $\lambda/20$ (λ is the wavelength). But the numerical size of this true 3D problem grows rapidly with the size of the crystal. On our workstation (640 MB of memory), the crystal size limit is about $5 \times 5 \times 5$ elementary cubic cells.

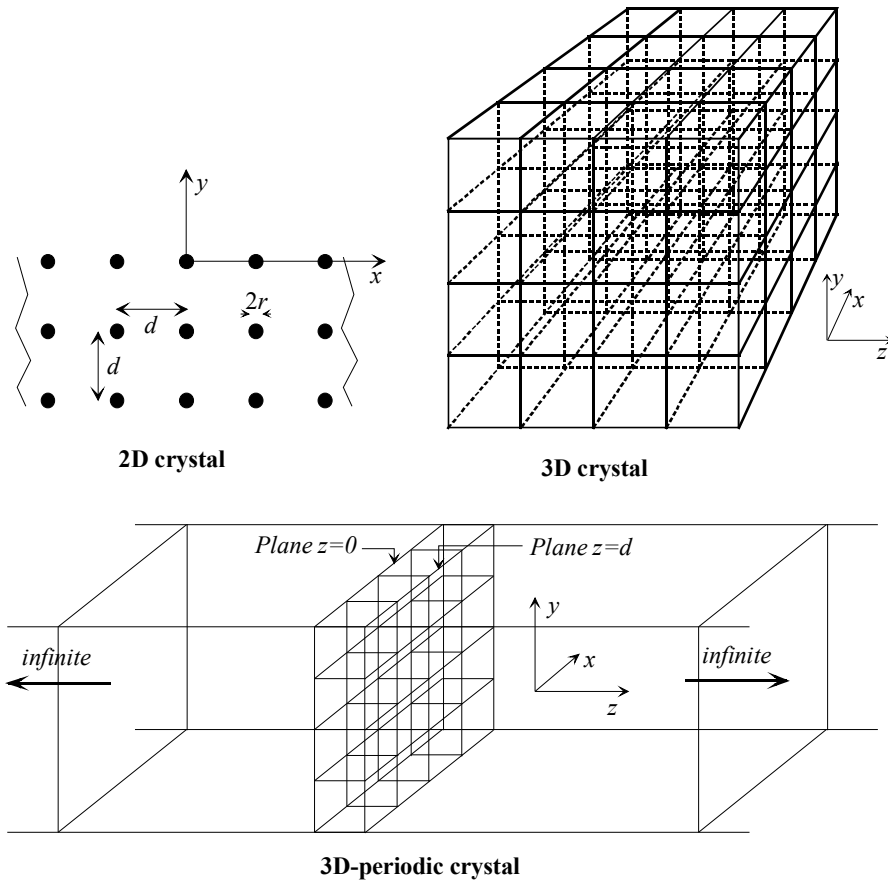


Figure 1. The 2D crystal is made of infinitely long parallel wires. It can be limited along the x direction (finite number of rods), or infinite along this direction. In this case, it becomes a grating composed of N_g grids ($N_g = 3$ on this figure). The 3D crystal depicted here is made of $4 \times 4 \times 4 = 64$ elementary cubic cells with edge d . The 3D-periodic crystal is limited in the x and y directions. It is composed of elementary cubic cells with edge d , and is periodic (and infinite) along the z direction with period d . For clarity, only one slice of cells is represented here.

In the case of the 3D-periodic crystal, we assume periodicity along the z direction. If the incident field is a plane wave (whatever its wave vector and its polarization), all the information is contained in the slice $z \in [0, d[$. We use the same theory as for the 3D crystal, but we replace the free space Green's function $\exp(ikR)/R$ with a Green's function taking into account the periodicity. This Green's function is now a series, whose terms can be expressed as Hankel functions in order to ensure a fast convergence of the series. Due to the reduced number of unknowns, we are able to deal with much larger structures than in the 3D problem: on the same computer,

crystals whose cross section is composed of 20×8 elementary cubic cells in the x,y plane become affordable.

2.2 Homogenization in the two-dimensional case

Our aim is to show the similarities and the differences in the behavior of these structures. It has been suggested [1,2] that these metallic crystals can simulate a homogeneous material having a plasmon frequency in the microwave domain. More precisely, and assuming E// polarization case (electric field parallel to the wires), it has been shown from a mathematical point of view that when the wavelength λ tends to infinity, the relative permittivity of the homogenized material can be easily deduced from the crystal parameters from the following formulas:

$$\varepsilon = 1 - \frac{\omega_p^2}{\omega^2} = 1 - \frac{\lambda^2}{\lambda_p^2} \quad (1)$$

$$\lambda_p = d \sqrt{2\pi \ln\left(\frac{d}{2r}\right)} \quad (2)$$

The preceding formulas imply that for very large λ , the permittivity is negative, and the optical index is a pure imaginary number. It means that the only solutions for the field in the crystal are evanescent, and no propagation can occur.

It is worth noting that in the H// polarization case (magnetic field parallel to the wires), and for the thin wires considered in this paper, there is no interaction between the incident field and the wires. Let us give a very simple explanation, which has nevertheless proved to be relevant in the interpretation of these crystals properties. This interaction is governed by the electric field, which moves the free charges in the metallic wire. In contrast with the E// case, the electric field in the H// case is perpendicular to the wires, and the charges are not able to move in this direction due to the small diameter of the wires.

Figure 2 shows the transmission of a 2D metallic photonic crystal illuminated in normal incidence by an E// polarized plane wave, for increasing numbers of grids. The filtering property for large wavelengths clearly appears, and we see that the transmission decreases exponentially with the number of grids, i.e. with the thickness of the crystal. We also observe a small gap centered on $\lambda = 1.8$. Note that it has been shown that the low-frequency gap of a metallic crystal is not a consequence of its

periodicity [11]. In this reference, the study concerns 2D crystals, but the result should hold for 3D crystals as well.

The most interesting feature of this set of curves is to show that the cut-off wavelength (whose value is around 5) is equal to the value given by (2). It suggests that the set of equations (1) and (2), established in the limit case $\lambda \rightarrow \infty$ could stay pertinent in the whole range of interest of these crystals, i.e. from the cut-off to the static limit.

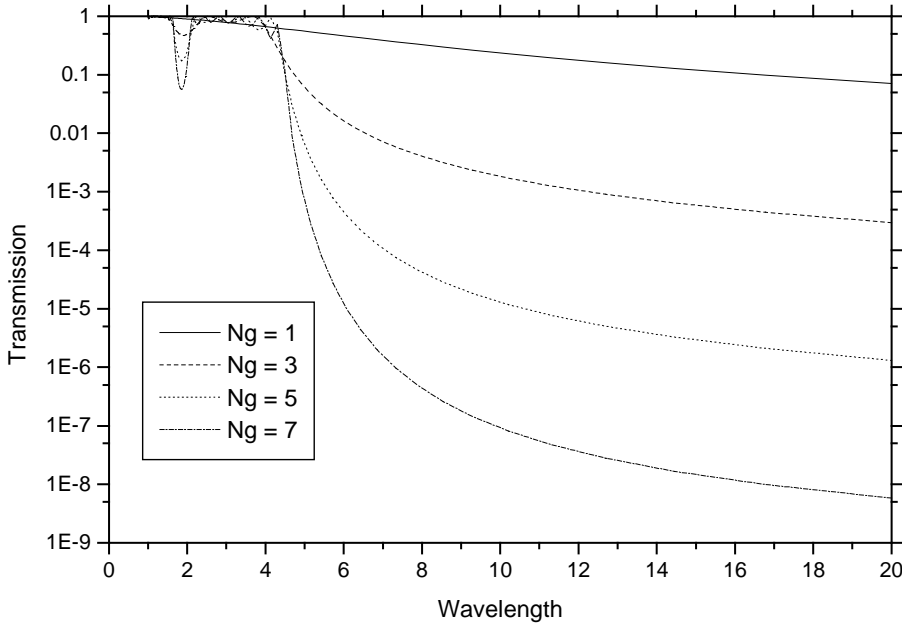


Figure 2. Transmission of a 2D metallic photonic crystal with infinite extent in the x direction and made of N_g grids, illuminated in normal incidence and $E//$ polarization. $d = 1$, $r = 0.01$.

Many numerical experiments have been performed in order to get more details on this conjecture [12]. We have considered the case of infinite gratings made of grids, studied the influence of the number of grids, of the incidence, of the radius of the wires. We also have considered the case where the wires lay in a finite region. From this work, we get the following conclusions. In the case of 2D metallic crystals made of thin wires with periodic square arrangement, and in the $E//$ polarization case:

- There exists a cut-off value given by (2) with quite good accuracy.
- In a range of wavelengths going from slightly less than the cut-off value to infinity, the crystal behaves as a homogeneous material whose

permittivity can be represented by (1) with good approximation. Note that it means that its effective optical index is real (and less than unity) for wavelengths less than the cut-off value and pure imaginary otherwise (which is in some sense obvious from energy considerations).

- The homogenized material is a little bit larger than the crystal itself. In fact, the limits of the homogenized material are obtained from the actual limits of the crystal by a translation of $d/2$.

In H// polarization, the crystal is transparent.

Let us illustrate on a simple example how these conclusions can be used. We consider in figure 3 two photonic crystals made of 3 grids (with infinite extent along the x -axis). According to the preceding rules, we can replace this structure by two homogeneous layers whose permittivity is given by (1). From the previous remarks, these two layers have a thickness equal to $3d$, and the distance between the layers is $3d$. Figure 4 shows the transmission of the two structures when they are illuminated in normal incidence by an E// polarized plane wave. Of course, the agreement is not perfect. Specially, it is surprising to notice the discrepancy of a factor around ten even for large wavelengths. In fact, it should be noticed that, even though the homogenization is an asymptotic process for large wavelengths, the crystal of figure 3 is made of two layers of three grids only. Of course, the validity of the homogenization requires the size of the object to be much greater than the size of the elementary cell of the crystal. Nevertheless, the homogenized structure allows us to predict qualitatively the behavior of the stack of grids, and quantitatively the location of the peaks.

Some other examples have also been studied, and in particular the case of a finite set of wires lying inside a circle [12]. We are led to the same conclusions, i.e. that the set of wires can be replaced by a homogeneous circular rod having the same diffraction properties.

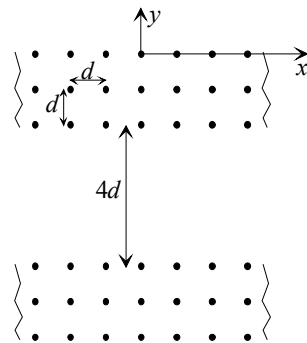


Figure 3. Two crystals made of 3 grids. The wire spacing is $d = 1$. The distance between the two crystals is $4d$. The radius of the wires is $r = 0.01$.

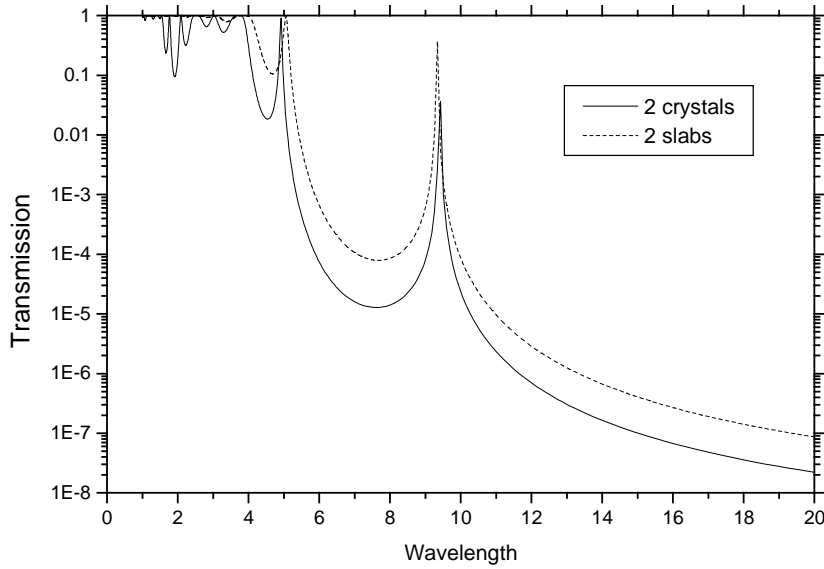


Figure 4. Transmission of the structure shown in figure 3 (solid line) and of the homogenized structure (dashed line).

2.3 Comparison between two-dimensional and three-dimensional cases

In the case of three-dimensional crystals, the basic idea is to say that, since the crystal is made of wires parallel to the 3 principal directions of space, the behavior of these crystals is less sensitive regarding the incidence conditions and the polarization. Indeed, whatever the direction of the incident wave vector, and whatever the polarization, there are always some wires in the 3D mesh which interact with the electromagnetic field. This prediction has been confirmed by our numerical investigations. Since there is no simple way to define a transmission in the case of a 3D bounded object, we define a quantity related to the penetration of the field inside the crystal. For this purpose, we compute a mean value of the electromagnetic energy, on several points close to the centre of the crystal. Figure 5 compares this quantity for several structures:

- 2D crystal composed of 5×5 parallel wires, normal incidence, $E//$ polarization,
- 3D crystal composed of $4 \times 4 \times 4$ cubic cells, normal incidence, electric incident field parallel to one of the wires directions,

- 3D-periodic crystal whose xy section is composed of 20×4 cubic cells (20 along x and 4 along y), electric incident field $\mathbf{E}^i = \exp(-iky) \mathbf{e}_z$ (see figure 1),
- Same crystal, but $\mathbf{E}^i = \exp(-iky) \mathbf{e}_x$,
- Same crystal, but $\mathbf{E}^i = (-2\mathbf{e}_x - \mathbf{e}_y + 2\mathbf{e}_z)/\sqrt{9} \exp(i\mathbf{k}^i \cdot \mathbf{r})$, and $\mathbf{k}^i = k(-\mathbf{e}_x - 2\mathbf{e}_y - 2\mathbf{e}_z)/\sqrt{9}$.

Figure 5 shows that the penetration inside the crystal has the same behavior in these different cases. Note that in the last case, the energy is lower, which can be attributed to the fact that the incident wave vector \mathbf{k}^i is not normal to the crystal. In all cases, the cut-off wavelength is close to 5, which is the value given by (2).

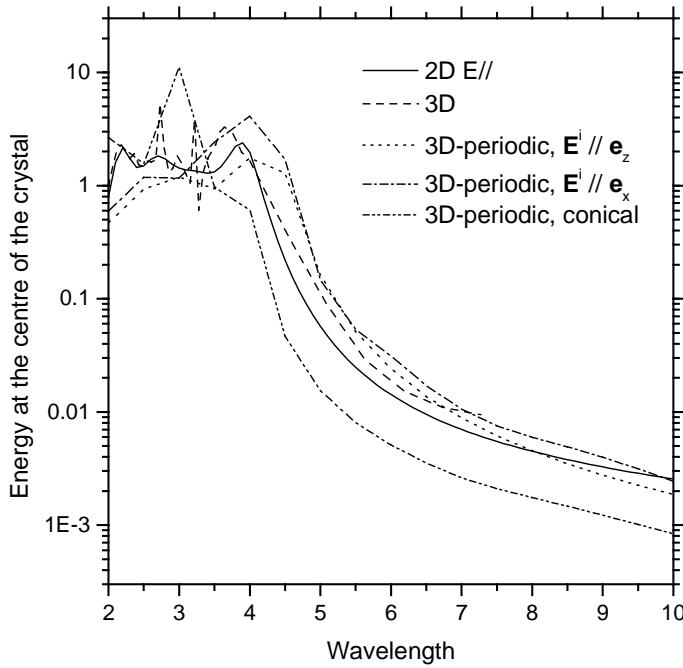


Figure 5. Energy at the centre of the crystal for several structures (details in the text).

Let us consider now a 3D-periodic crystal as depicted in figure 1, with a xy cross section made of 20×8 cubic cells. Figure 6 shows the field maps for two different polarization cases. In the upper map where the electric incident field is parallel to the z -axis, the screening property of the crystal is evident. The lower map (electric incident field parallel to the x -axis) shows two features. First, the value of the field inside the crystal is about the same as in

the upper map, which confirms the previous paragraph results. Second, there is clearly no shadow below the crystal. The difference between these two cases is due to the intensities flowing in the wires. In the case of the upper map, all the intensities flow along the wires parallel to the z -axis (computations show that the intensities along the other wires are insignificant). Intensities only take significant values on the upper face of the crystal, and decrease rapidly inside the crystal. In the case of the lower map, the intensities are inclined to flow along the wires parallel to the x -axis. Since the crystal is limited in this direction, we numerically observe that they actually flow in the plane of the figure, but on the entire boundary of the crystal. That is why they radiate a field all around the crystal. This property, which is due to the finite size of the crystal, should be kept in mind in the prospect of screening applications involving metallic photonic crystals.

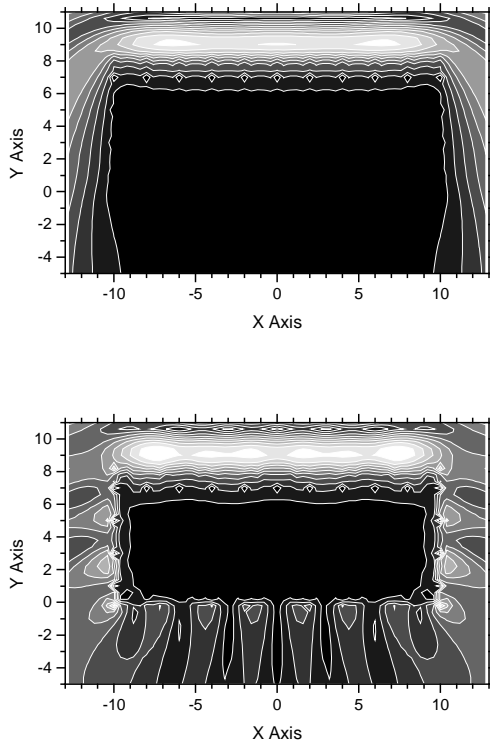


Figure 6. Modulus of the total electric field in the xy section a 3D-periodic crystal with 20×8 cubic cells. The crystal is located in the area $-10 \leq x \leq 10$ and $0 \leq y \leq 8$. It is illuminated in normal incidence by a plane wave with unit amplitude, coming from the top of the figures. The wavelength is $\lambda = 6$ (greater than the cut-off wavelength). Top: incident field parallel to the z -axis. Bottom: incident field parallel to the x -axis. The color maps are the same in both cases, going from black inside the crystal (modulus less than 0.2) to white (between 2 and 2.2). Crystal parameters: $d = 1$, $r = 0.01$.

3. ULTRAREFRACTION PROPERTIES OF 2D DIELECTRIC CRYSTALS

3.1 Presentation of the phenomenon

It has been suggested from dispersion diagrams that the phase velocity of Bloch waves inside an infinite photonic crystal could tend to infinity near the band edges [13-15]. Consequently, the crystal should have an effective optical index that tends to zero, and should exhibit strange ultrarefractive properties. In fact, this effective index depends on the direction of propagation; i.e. the equivalent homogenized structure is not isotropic. A detailed study of the dispersion diagrams in the Brillouin zone can bring some information on this effective index, but it is not in the scope of the present paper. We want here to study numerically and quantitatively the ultrarefractive phenomena, which may occur when a limited beam illuminates a finite crystal.

The crystal is a 2D structure (figure 1) made of dielectric circular rods with optical index 3, and lying in vacuum. The radius of the rods is $r = 0.475$, the square cell has a spacing $d = 1.27$. These parameters are those of the experimental study of Smith et al. [16]. In the present study, the crystal is made of 7 grids ($N_g = 7$). All the study concerns E// polarization (electric field parallel to the rods).

Figure 7 gives the dispersion relation of the infinite crystal computed with the plane waves expansion method [17]. We work near the full gap represented by the light dot lines. Since we consider incidences close to the normal (y -axis, which corresponds to the Γ -X region), the local gap appears to be wider, and the frequency of interest is pointed out by the dashed line ($d/\lambda \approx 0.5$). We remark that the group velocity is low in this region, as shown by the low slope of the dispersion curve. Note that there is another gap for greater wavelengths ($d/\lambda \approx 0.26$).

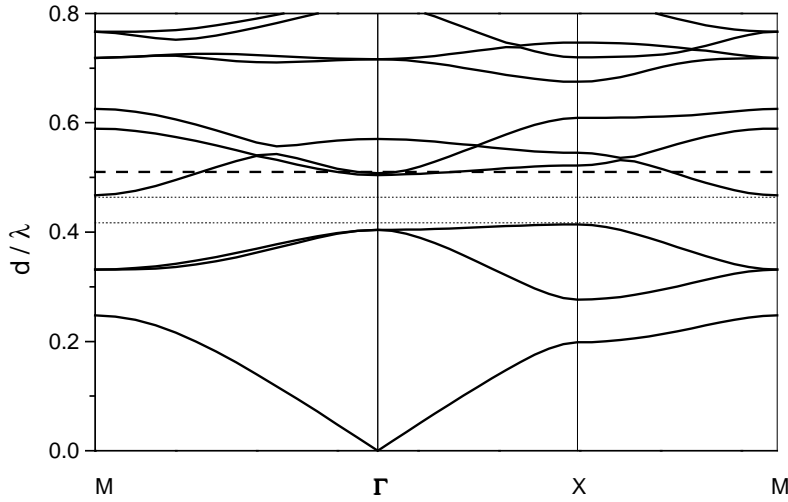


Figure 7. Dispersion relation for E// polarization in a 2D crystal with square lattice. The abscissa represents the Bloch wave vector in the Brillouin zone where Γ , X and M stand for $(0,0)$, $(\pi/d,0)$ and $(\pi/d,\pi/d)$.

3.2 Numerical analysis of the transmission of a plane wave

Since the phenomena occur at the band edge, let us study the transmission factor of the grating (infinite along the x direction) made of 7 grids. To this end, we use our grating code based on an integral theory [5]. The complex transmission factor in the zero grating order $t(\theta, \lambda)$ depends on the angle of incidence of the incident plane wave θ and on the wavelength. We plot in figure 8 the square of the modulus (transmitted energy) and the phase of $t(0, \lambda)$. Note that in the range of interest, the grating gives rise to only one propagating order. Figure 8 shows the shorter wavelengths band edge of the gap. The two peaks for $\lambda = 2.558$ and 2.545 will enable us to get a significant transmission of the beam. Note that for each of them, the phase shows a rapid variation.

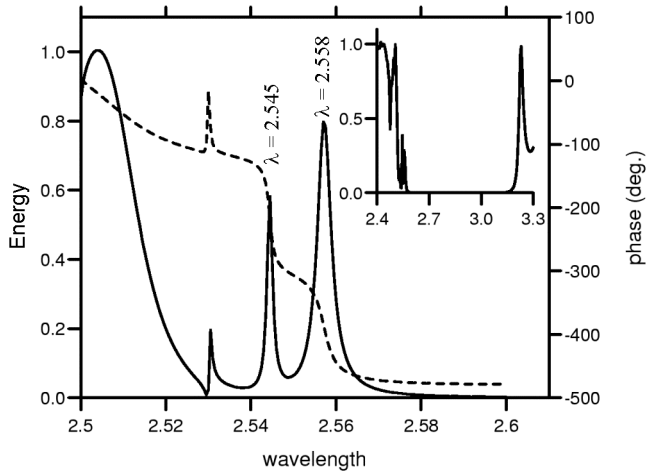


Figure 8. Energy (solid line) and phase (dashed line) of transmitted zero order. Normal incidence, E// polarization. The smaller inserted graph shows the energy on a larger range of wavelengths.

3.3 Anomalous shift and widening of a gaussian beam

In a simple and heuristic analysis, we can see the crystal as a homogeneous layer with low optical index. Consequently, we expect to exhibit two phenomena depicted in figure 9: the widening and the anomalous shift of a limited beam going through the crystal.

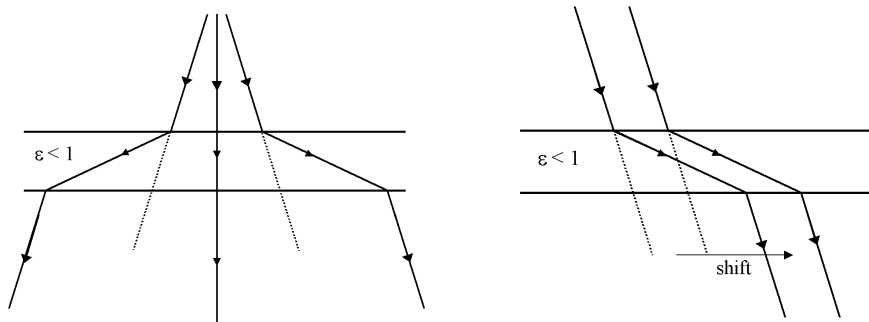


Figure 9. Schematic representation using Fresnel's law of the widening (left) and of the anomalous shift (right) of a beam going through a slice of low index material

From now on, we suppose that λ is fixed, and thus we omit the wavelength dependency. The incident limited beam is described by a gaussian plane waves packet:

$$E^{inc}(x, y) = \int_{-\infty}^{+\infty} A(\alpha) \exp(i\alpha x - i\beta(\alpha)y) d\alpha \quad (3)$$

where $\alpha = (2\pi \sin \theta) / \lambda$, $\beta(\alpha) = \sqrt{k^2 - \alpha^2}$. We consider a gaussian beam with width W and mean incidence θ_0 such as $\alpha_0 = (2\pi \sin \theta_0) / \lambda$:

$$A(\alpha) = \frac{W}{2\sqrt{\pi}} \exp\left(-\frac{(\alpha - \alpha_0)^2 W^2}{4}\right) \quad (4)$$

Putting $\tau(\alpha) = t(\theta, \lambda)$, the transmitted field is given by (the evanescent waves, which vanish rapidly around the crystal, can be neglected):

$$E^t(x, y) = \int_{-\infty}^{+\infty} A(\alpha) \tau(\alpha) \exp(i\alpha x - i\beta(\alpha)y) d\alpha \quad (5)$$

It means that the knowledge of $t(\theta, \lambda)$ is sufficient to get the transmitted field. It can be noticed that for $y = 0$, the transmitted field is the Fourier transform of $A(\alpha) \tau(\alpha)$. Equation (5) shows that the plot of $t(\theta, \lambda)$ for the fixed value of λ will bring us useful information on the transmitted field. This information, as well as the angular dependency of $A(\alpha)$, is given in figure 10, which shows that the product of $A(\alpha)$ by $\tau(\alpha)$ in (5) will narrow the angular range of waves in the transmitted packet, and consequently widen its Fourier transform, thus the spatial width of the transmitted beam. This widening is clearly observed in figure 11.

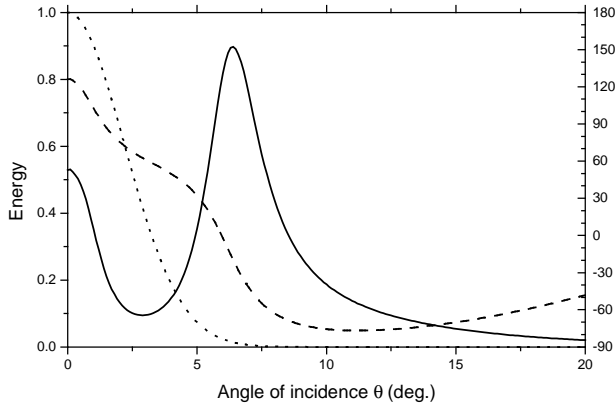


Figure 10. Transmitted energy (solid line) and phase (dashed line) of $t(\theta, \lambda)$ for $\lambda = 2.545$. The dotted line represents the exponential factor in equation (4).

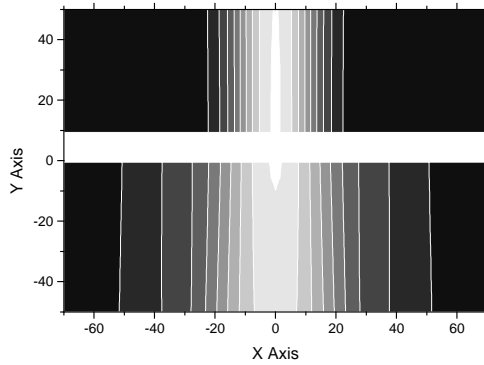


Figure 11. Widening of the beam: field map of the incident (above the crystal) and transmitted (below the crystal) field modulus. The transmitted field has been multiplied by a factor 2.25 in order to get the same maximum value as the incident field. $\lambda = 2.545$, normal incidence, $W = 15$. The white region corresponds to the crystal.

In order to observe an anomalous beam shift, let us change the mean incidence to $\theta_0 = 6.4^\circ$ corresponding to the second peak on figure 10. This phenomenon is very close to Goos-Hanschen effect that arises near the total reflection on a plane interface. As well known, the amplitude of this shift is linked to the fast variation of the reflection coefficient phase. In our case, the choice $\theta_0 = 6.4^\circ$ presents two interesting features: it brings a great transmitted energy, and offers a wide phase variation. The phenomenon is illustrated in figure 12.

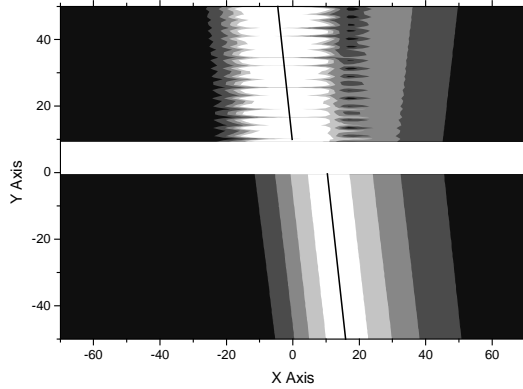


Figure 12. Anomalous beam shift: field map of the total field modulus. Same parameters as in figure 11, but $\theta_0 = 6.4^\circ$. Here, the transmitted field has not been normalized. The dark lines show the locus of the maximum incident and transmitted beams. We also see an interference pattern between the incident and the reflected fields.

CONCLUSION

In a first part of this paper, it has been shown from numerical results based on a theory of scattering from thin metallic wires that the formulae coming from mathematical studies of homogenization provides a precise estimate of the properties of metallic photonic crystals, even when the wavelength has the same order of magnitude as the period of the crystal. This property which could simplify considerably the numerical calculations is all the more interesting since it extends to doped crystals.

In a second part we have confirmed from numerical calculations the phenomenon of ultrarefraction generated by photonic crystals at the edges of a gap.

ACKNOWLEDGMENTS

The work described in this paper has been done under a contract between the Laboratoire d'Optique Électromagnétique and the Direction Générale de l'Armement (French Ministry of Defense).

REFERENCES

- [1] J.B. Pendry, A.J. Holden, W.J. Stewart, and I. Youngs, "Extremely low frequency plasmons in metallic mesostructures", *Phys. Rev. Lett.* **76**, 4773-4776 (1996).
- [2] D. Felbacq and G. Bouchitté, "Homogenization of a set of parallel fibers", *Waves in random media* **7**, 245-256 (1997).
- [3] R.C. McPhedran, C.G. Poulton, N.A. Nicorovici and A.B. Movchan, "Low frequency corrections to the static effective dielectric constant of a two-dimensional composite material", *Proc. R. Soc. Lond. A* **452**, 2231-2245 (1996).
- [4] R.C. McPhedran, N.A. Nicorovici and L.C. Botten, "The TEM mode and homogenization of doubly periodic structures", *J. Electrom. Waves and Appl.* **11**, 981-1012 (1997).
- [5] D. Maystre, "Electromagnetic study of photonic band gaps", *Pure Appl. Opt.* **8**, 875-993 (1994).
- [6] D. Felbacq, G. Tayeb and D. Maystre, "Scattering by a random set of parallel cylinders", *J. Opt. Soc. Am. A* **11**, 2526-2538 (1994).
- [7] G. Guida, D. Maystre, G. Tayeb, and P. Vincent, "Electromagnetic modelling of three-dimensional metallic photonic crystals", *J. Electr. Waves and Appl.* **12**, 1153-1179 (1998).
- [8] S. Enoch, G. Tayeb and D. Maystre, "Numerical evidence of ultrarefractive optics in photonic crystals", *Optics Comm.* **161**, 171-176 (1999).
- [9] R. Harrington, "Matrix methods for field problems", *Proc. IEEE*, Vol. 55, No. 2, 136-149 (1967).
- [10] Numerical Electromagnetic Code (NEC), available on the internet, see for instance <http://www.qsl.net/wb6tpu/swindex.html>
- [11] G. Guida, "Numerical study of band gaps generated by randomly perturbed bidimensional metallic cubic photonic crystals", *Optics Comm.* **156**, 294-296 (1998).
- [12] G. Guida, D. Maystre, G. Tayeb and P. Vincent, "Mean-field theory of two-dimensional metallic photonic crystals", *J. Opt. Soc. Am. B* **15**, 2308-2315 (1998).
- [13] J.P. Dowling and C.M. Bowden, "Anomalous index of refraction in photonic bandgap materials", *Journal of Modern Optics* **41**, 345-351 (1994).
- [14] P. M. Visser, G. Nienhuis, "Band gaps and group velocity in optical lattices", *Optics Comm.* **136**, 470-479 (1997).
- [15] R. Zengerle, "Light propagation in singly and doubly periodic planar waveguides", *J. Mod. Optics* **34**, 1589-1617 (1987).
- [16] D.R. Smith, S. Schultz, S.L. McCall, P.M. Platzmann, "Defect studies in a two-dimensional periodic photonic lattice", *Journal of Modern Optics* **41**, 395-404 (1994).
- [17] M. Plihal and A.A. Maradudin, "Photonic band structure of two-dimensional systems: the triangular lattice", *Phys. Rev. B* **44**, 8565-8571 (1991).